Structure and Dynamics of Poly(*n*-decyl methacrylate) below and above the Glass Transition

G. Floudas*

Foundation for Research and Technology-Hellas (FORTH) Institute of Electronic Structure and Laser P.O. Box 1527, 711 10 Heraklion, Crete, Greece

P. Štepánek

Institute of Macromolecular Chemistry, Academy of Sciences of the Czech Republic 16206 Prague, Czech Republic

Received March 24, 1998; Revised Manuscript Received July 17, 1998

ABSTRACT: The structure and dynamics of the "strong" glass of poly(*n*-decyl methacrylate) (PnDMA) have been studied, respectively, with X-ray diffraction and dielectric spectroscopy, dynamic light scattering, and rheology at temperatures below and above the glass transition temperature $T_g \sim 215$ K. We find three dielectrically active processes, starting from low temperatures: (i) the γ-relaxation deep into the glassy state (with an activation energy of 5.7 kcal/mol), (ii) the "fast" β-relaxation just above the calorimetric T_g, with an activation energy of 11.4 kcal/mol, and (iii) the mixed $\alpha\beta$-relaxation which has many similarities to a single α-process. Dynamic light scattering also identified the last two processes. The distribution of relaxation times for the $\alpha\beta$-relaxation exhibits a strong T dependence ranging from a Kohlraush−Williams−Watts (KWW) parameter of 0.25 at T_g to about 0.7 at $T_g + 115$ K. This strong T dependence, which is a common feature of poly(*n*-alkyl methacrylates) with long side chains, reflects the contributions from concentration fluctuations from the PMMA-like backbone and the PE-like side chain. We compare our structural and dynamic results with those from the other members of the poly(*n*-alkyl methacrylates) series. There is a pronounced dependence of the fragility or steepness index on the length of the alkyl side chain. We found that this dynamic property has its origin on the low van der Waals peak (LVDW) of the static structure factor and reflects mainly differences in intersegmental distances and packing.

Introduction

Liquids are classified as "fragile", "strong", or intermediate.[1] The term "fragility" was introduced by Angell to describe the stability of the short- and medium-range order against temperature-induced degradation. Fragile liquids are usually liquids without directional bonds and very often have ionic or aromatic character. Strong liquids are usually those with self-reinforcing tetrahedral network structures which show a small change in heat capacity at the glass transition temperature, T_g. More recently,[2] a connection between fragility with the topology of the potential energy surface was proposed. The relation reflects on the density of minima of the potential energy surface. According to this property, strong liquids are those with a small number of minima at any temperature above the ground-state energy. This property together with the Adam−Gibbs theory for the viscosity results in a more Arrhenius behavior for the viscosity $\eta(T)$ (or the relaxation time $\tau(T)$). Alternatively, fragile liquids are those with a large number of distinct minima which show deviations from the Arrhenius behavior.

This "fragile" or "strong" behavior of liquids is usually depicted in a plot of the relaxation times as a function of T_g/T. Recently,[3] a large number of polymers have been compared and a large variation of the curvature was found in the "cooperativity plot" (i.e. $\log \tau$ vs T_g/T). The term "cooperativity" was chosen to reflect the capacity of intermolecular coupling, which varies from one polymer to the other depending on the chemical structure. In fact, the curvature or steepness of the relaxation times in the T_g-scaled plot, evaluated at $T = T_g$, was found to increase in the same order as the value of $n^* = 1 - \beta_{KWW}$, where β_{KWW} is the Kohlrausch−Williams−Watts (KWW) exponent. Notwithstanding the big success of this correlation in many glass formers, no reliable prediction of fragility from the structural characteristics alone is possible in complex polymeric systems.

One might hope, however, that, within a certain family of polymers, the small change of the structural unit from one member to the other could reflect on the dynamic behavior (fragile vs strong), and in this way it might be possible to trace the difference in dynamics back to the structure. Poly(*n*-alkyl methacrylates) is one such example, where by changing the length of the alkyl side chain (l) one affects strongly the dynamic response of the system. We have shown in an earlier study[4] of poly(*n*-lauryl methacrylate) (PnLMA) ($l = 12$) that this is indeed the case: by increasing l, we are going from the "fragile" poly(methyl methacrylate) (PMMA) to the "strong" glass of PnLMA. Poly(*n*-alkyl methacrylates) have been the subject of intense rheological,[5,6] dielectric,[4,7−16] light scattering,[17−21] and more recently NMR[22] investigations. From these studies, the shift of the glass transition to lower temperatures with increasing l (an effect known as internal plasticization) as well as the existence of secondary processes in the glass are well documented. In particular, the splitting and interplay[12] between the primary α-relaxation and the "slow" β-relaxation with temperature and pressure[9,10] have been extensively studied. Because of the low-frequency merging of the primary (α-relaxation) and "slow" β-relaxation (we use the term "slow" to differentiate from the "fast" β-relaxation discussed below) with increasing l, we are practically studying the mixed ($\alpha\beta$)

S0024-9297(98)00460-4 CCC: $15.00
Published on Web 09/10/1998

relaxation which bears many similarities to the segmental (α) process.

The purpose of the present study is to shed light on the structure vs dynamics relationship of fragile/strong liquids. For this purpose we employ the series of poly(*n*-alkyl methacrylates), and we study in detail the structure and dynamics of a specific member of the series, poly(*n*-decyl methacrylate) (PnDMA), which is composed of a long alkyl side chain ($l = 10$). The structure has been investigated with wide-angle X-ray scattering (WAXS) for the members of the series with $l \leq 12$. The dynamics have been investigated with dielectric spectroscopy, rheology and dynamic light scattering. We find that the pronounced dependence of the fragility on l is reflected in changes of the static structure factor on the length scale of the intersegmental distances. Poly(*n*-alkyl methacrylates) form a family of polymers where one can associate the dynamic response with the chemical structural changes.

Experimental Section

Sample. Decyl methacrylate monomer (Polysciences, Inc.) was distilled under vacuum into a dust-free light scattering cell. The cell was flame-sealed under vacuum and the monomer thermally polymerized for 36 h at 393 K. The sample was then annealed an additional two weeks at 373 K to reach equilibrium and then slowly cooled-down to room temperature over a period of several days. The weight-average molecular weight $M_w = 1.65 \times 10^5$, was determined, after dissolution in tetrahydrofurane, by static light scattering using a Zimm diagram. The refractive index increment, $dn/dc = 0.0765$ was measured with a Brice Phoenix differential refractometer. The polydispersity index $M_w/M_n = 2.5$ was determined by dynamic light scattering on the same dilute solution using a Pearson fit to the correlation function, $g^1(t) = (1 + t/\tau_o)^{-p}$. The polydispersity index is then given by $M_w/M_n = \Gamma(p)\Gamma(p + 2/\nu)/\Gamma^2(p + 1/\nu)$, where Γ is the gamma function and ν is the Flory exponent ($\nu = 0.6$ was used as appropriate for solutions in good solvents); this procedure is fully described in refs 23 and 24.

Differential Scanning Calorimetry (DSC). The glass transition temperature T_g was measured with a DSC. The sample was first cooled to 120 K (cooling rate 15 K/min), and a thermogram was taken while heating to 373 K (heating rate 20 K/min). A second thermogram was taken after cooling to 120 K (cooling rate 15 K/min) and subsequent heating (heating rate 10 K/min). A very broad transition was found centered around 215 K with a breadth $\Delta T_g \sim 50$K. In Figure 1, the T_g's of the different poly(*n*-alkyl methacrylates) with $l \leq 12$ are shown from pressure−volume−temperature (PVT) measurements[25] and DSC (the DSC data for PnPMA and PnOMA are from ref 26). The line is a fit to the DSC data according to $T_g = 397 - 27.12l + 0.996l^2$. Evidently, the lower members of the series are more effective in reducing the glass transition (internal plasticization) as compared to PnLMA.

Wide-Angle X-ray Scattering (WAXS). A Siemens $\theta-\theta$ diffractometer (D500T) was used in the reflection geometry as described elsewhere in detail. Measurements were made in the Q-range 1−26 nm^{-1} and for different temperatures in the range 223−293 K. Figure 2a shows the WAXS spectrum of PnDMA compared to other members of the poly(*n*-alkyl methacrylate) series at 293 K. In Figure 2b, the PnDMA spectra are shown at two temperatures. The arrows indicate the positions of the three main peaks. The data were not corrected for the different sample volumes; therefore, the scaling on the *y*-axis of Figure 2 is arbitrary.

Dynamic Light Scattering (DLS). The autocorrelation function of scattered light was measured using an ALV5000/E multibit, multi-τ correlator. The light source was a Coherent Innova 70 argon-ion laser operated at 514 nm. Measurements have been made in the depolarized geometry (VH). A vertically (V) oriented Glan-Thompson polarizer was inserted into the incident laser beam and a horizontally (H) oriented Glan-Thompson polarizer in the scattered beam. The extinction ratio of the polarizers was better than 10^{-5}. Scattered light was collected at an angle of 90° by means of an optical fiber and detected by the ALV PIPD double detector operated in the pseudo-cross-correlation mode. This ensured elimination of correlation function distortions at short delay times. The sample was placed in an index matching liquid in a temperature-controlled sample holder. Cooling was achieved by circulation of nitrogen vapors through the sample holder that had been obtained by boiling liquid nitrogen. Fine tempera-

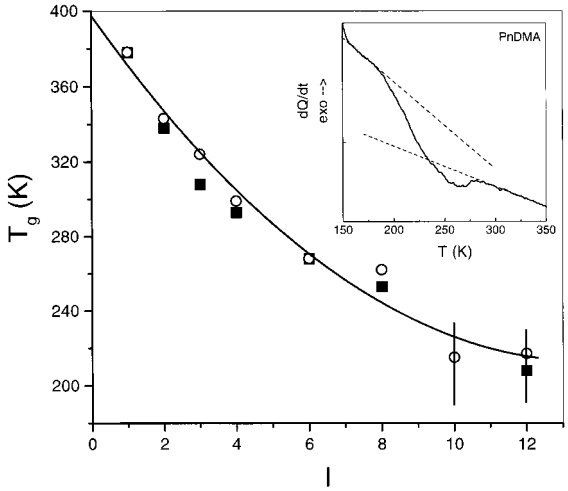

Figure 1. Glass transition as a function of the number of carbon atoms (l) on the side chain of poly(*n*-alkyl methacrylates). The two data sets are from PVT (■) and DSC (○). The vertical lines for PnDMA and PnLMA indicate the breadth of the transition obtained from DSC. In the inset the DSC trace of PnDMA is shown.

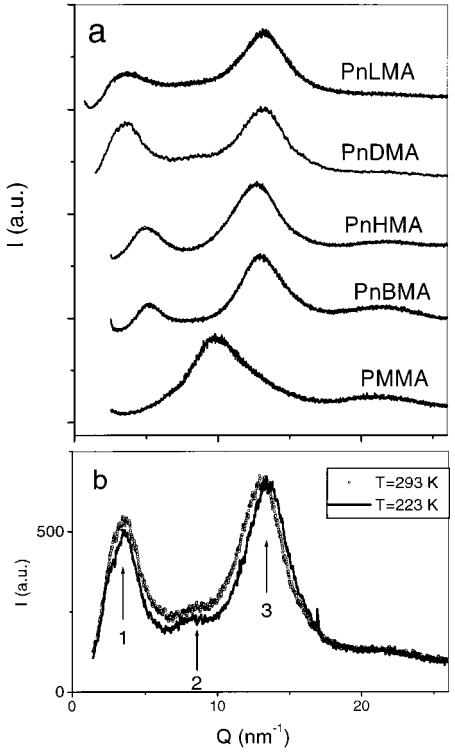

Figure 2. (a)Wide-angle X-ray scattering spectra of a series of poly(*n*-alkyl methacrylates) shown at 293 K. Notice the development of the low van der Waals (LVDW) peak which shifts to lower Q values with increasing alkyl side chain. (b) WAXS spectra for PnDMA shown at two temperatures as indicated. Arrows show the positions of the three main peaks in the spectra.

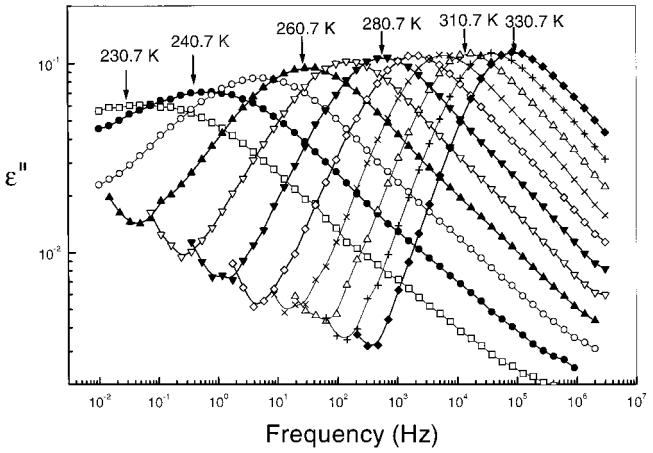

Figure 3. Dielectric loss plotted as a function of frequency for several temperatures as indicated. Notice that the distribution of relaxation times narrows with increasing temperature.

ture adjustments have been ensured by a computer-controlled temperature controller. A stream of nitrogen prevented condensation on the cell windows.

Dielectric Spectroscopy (DS). Measurements of the complex dielectric function have been made with a Novocontrol BDC−S system composed of a frequency response analyzer (Solartron Schlumberger FRA 1260) and a broad band dielectric converter with an active sample cell. The latter contains six reference capacitors in the range from 25 to 1000 pF. Measurements were made in the frequency range from 10^{-2} to 10^6 Hz using a combination of three capacitors in the active sample cell. The resolution in tan δ was 2×10^{-4} in the frequency range between 10^{-1} and 10^5 Hz. The sample was kept between two gold-plated stainless steel plates of 20 mm diameter with a separation of 100 μm maintained by Teflon spacers. Care was taken so that the sample (which is liquid at room temperature) filled homogeneously the volume between the electrodes. The sample cell was then set in the cryostat and the sample temperature was controlled between 173.2 and 330.7 K and measured with a PT100 sensor in the lower plate of the sample capacitor with an accuracy of 0.1 K. Typical dielectric loss data at some temperatures are shown in Figure 3.

Rheology. Measurements of the complex shear modulus G^* were made with a Rheometrics RMS800 spectrometer and for 16 temperatures within the range from 210 to 345 K and for 10 frequencies in the range from 0.1 to 100 rad/s.

Data Analysis. WAXS. The WAXS spectra of semicrystalline samples show sharp diffraction peaks whose intensities and widths reflect the frequencies and periodicities, respectively, of some characteristic distances obtained using Bragg's law: $d = 2\pi/Q^*$. For "amorphous" polymers the lack of sharp diffraction peaks makes the assignment of a Bragg spacing from the position of a scattering maximum only a crude approximation. Hence, in amorphous polymers we can only speak about the *equivalent* Bragg spacings. With the exception of PMMA, the WAXS spectra for poly(*n*-alkyl methacrylates) show three peaks (arrows 1, 2, and 3 in Figure 2b). The peak at high Q, with an equivalent Bragg spacing of about 5 Å, corresponds to the van der Waals (VDW) contacts of atoms and is known as the VDW peak. The temperature variation of this peak reflects mainly the thermal expansion of the system.[27] The peak at low Q, which is usually referred as the low van der Waals (LVDW) peak, is found to have a systematic dependence in the number (l) of carbon atoms on the alkyl side chain. Figure 4 displays the dependence of the three peaks on $l^{1/2}$ for a series of poly(*n*-alkyl methacrylates) with l in the range from $1 \le l \le 12$, at 293 K. The LVDW peak, with corresponding distances from 10 to 18 Å, reflect mainly the average distance between adjacent backbones which is an increasing function of the number of carbon atoms l on the alkyl side chain. The l-dependence of d_1 can be parametrized

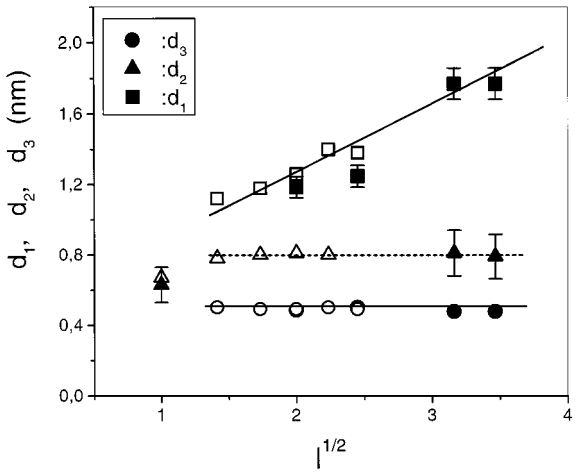

Figure 4. Equivalent Bragg spacings as a function of the number of carbon atoms (l) on the alkyl chain. Lines are linear fits to the data. Key: open symbols, from ref 28; filled symbols, this work. Notice the pronounced l-dependence of d_1 (low-Q peak in Figure 2).

as $d_1 = d_o + sl^{1/2}$, with $d_o \approx 0.7$ nm and $s \approx 0.385$ nm/CH_2. The intermediate peak (peak 2), which is more difficult to obtain, is also plotted in Figure 4. Its position corresponds to the main peak in PMMA which, in contrast to the rest of the series, does not exhibit a LVDW peak. This feature of PMMA has been discussed in the literature earlier.[28]

Dielectric Spectroscopy (DS). The complex dielectric permittivity $\epsilon^* = \epsilon' - i\epsilon''$, where ϵ' is the real and ϵ'' the imaginary part, was measured as a function of frequency and temperature. There are two principal mechanisms which contribute to ϵ^* in our system: orientation polarization of permanent dipoles (ϵ^*_{dip}) and dc conductivity (ϵ^*_{dc}):

$$\epsilon^* = \epsilon^*_{dip} - i\frac{\sigma_{dc}}{\epsilon_o \omega} \tag{1}$$

In the second term, σ_{dc} is the dc-conductivity and ϵ_o (=8.854 pF/m) is the permittivity of free space. The electrical conductivity in the sample causes the increase of the dielectric loss at low frequencies (Figure 3) and is fitted according to $\epsilon'' \sim (\sigma_{dc}/\epsilon_o)\omega^{-1}$. The orientational contribution was fitted using the empirical function of Havriliak and Negami (HN)[29]

$$\frac{\epsilon^*_{dip}(\omega) - \epsilon_\infty}{\Delta\epsilon} = \frac{1}{[1 + (i\omega\tau_{HN})^\alpha]^\gamma} \tag{2}$$

where τ_{HN} is the characteristic relaxation time in this equation. The parameters α and γ describe, respectively, the symmetrical and asymmetrical broadening of the distribution of relaxation times and $\Delta\epsilon$ (=$\epsilon_o - \epsilon_\infty$) is the relaxation strength of the process under investigation.

With DS we found three dielectrically active processes. Starting from low temperatures, in the range $170 < T < 190$ K we have the γ-relaxation, in the range $240 < T < 280$ K two processes could be resolved, and the "fast" and "slow" processes were identified, respectively, with the "fast" β- and primary ($\alpha\beta$) relaxations. Within this T range we have used two HN functions to fit the experimental spectra. Figure 5 shows a representative fit to the dielectric loss spectrum at 260.7 K using two HN functions. Notice the small intensity of the fast process which is 1/10 of that of the main process due to the primary ($\alpha\beta$) relaxation. In the range $280 < T < 330$ K, the fast process was too fast to be observed within the experimental window, and a single HN function was adequate in representing the experimental data.

As an alternative fitting procedure to the use of two HN functions within the T range $240 < T < 280$ K, we have employed an approach which makes no assumption on the form of the relaxation function. This approach is based on

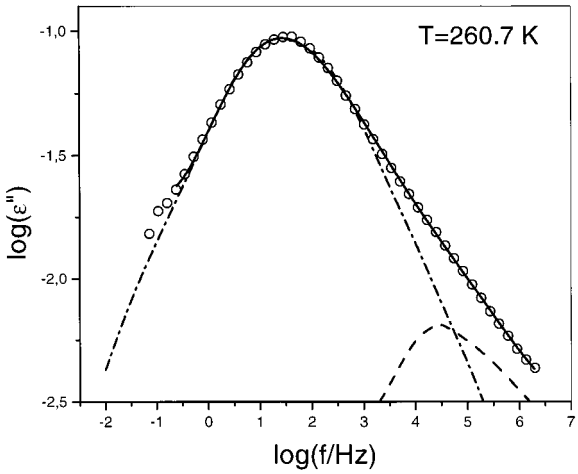

Figure 5. Fit of the dielectric loss data of PnDMA at 260.7 K using a double HN function. The "fast" and "slow" processes correspond to the β- and α-relaxations, respectively.

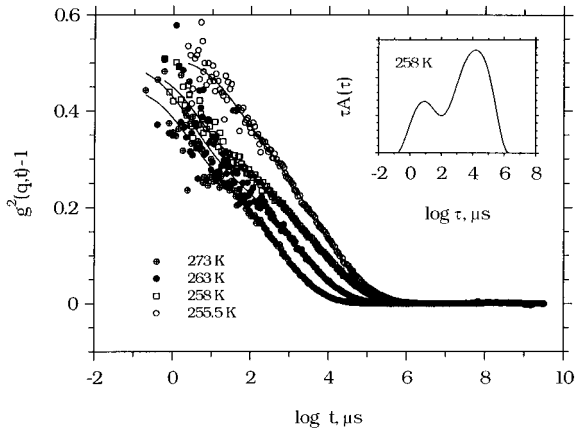

Figure 6. Measured correlation functions for PnDMA taken in the VH geometry at a scattering angle of 90°: (⊕) 273; (●) 263; (□) 258; (○) 255.5 K. The inset shows the distribution of relaxation times at the temperature of 258 K.

the inversion of the dielectric data using CONTIN[30]

$$\frac{\epsilon''(\omega)}{\Delta\epsilon} = \int_{-\infty}^{+\infty} G(\tau)\frac{\omega\tau}{1+(\omega\tau)^2}\,\mathrm{d}(\ln\tau) \tag{3}$$

and provides directly the distribution of relaxation times $G(\tau)$. The relaxation times obtained from this approach were nearly identical to the approach based on the HN fitting function.

Dynamic Light Scattering (DLS). Figure 6 shows intensity correlation functions $g_{VH}^2(t)$ obtained at various temperatures in the range 273−255.5 K. As with DS, within the investigated T range, two decay processes are present in the DLS spectra which are easier to observe in the corresponding distributions $A(\tau)$ of relaxation times τ (shown in the inset at 258 K), obtained by applying the inverse Laplace transformation[31,23] to the field correlation function $g_{VH}^1(t) = (g_{VH}^2(t) - 1)^{0.5}$:

$$g_{VH}^{\ 1}(t) = \int_0^\infty A(\tau)\exp(-t/\tau)\,\mathrm{d}\tau \tag{4}$$

To quantitatively assess both the positions and widths of the two peaks, we have consistently fitted the field correlation functions with a double KWW function[23]

$$g_{VH}^{\ 1}(t) = A_f e^{-(t/\tau)^{\beta_f}} + A_s e^{-(t/\tau)^{\beta_s}} \tag{5}$$

where β_f and β_s describe the widths of the fast and slow relaxation modes, A_f and A_s being their amplitudes.

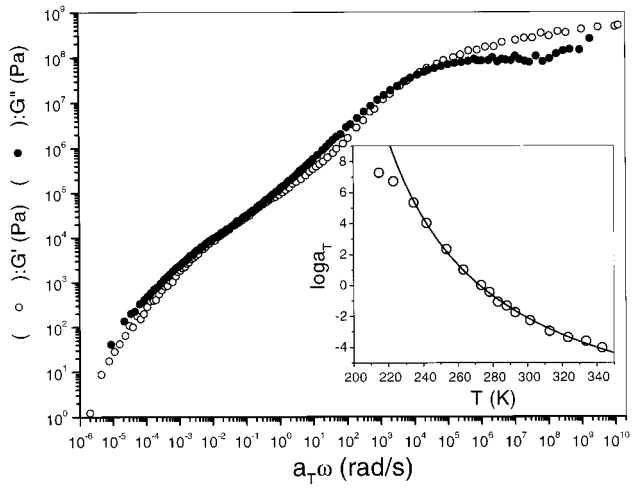

Figure 7. Reduced frequency plot for the storage (G') and loss (G'') moduli of PnDMA using $T_o = 272.5$ K as the reference temperature. The shift factors used for the time−temperature superposition are plotted in the inset. The solid line is a fit to the WLF equation (see text).

Rheology. The storage G' and loss G'' moduli were shifted on the horizontal axis, the master curves were constructed using the principle of time−temperature superposition, and the result is shown in Figure 7. The reference temperature was 273.6 K and the shift factors used in the shifting procedure are shown in the insert. The shifted G' and G'' data exhibit a broad glass−rubber relaxation at high frequencies followed by a short entanglement plateau and by the flow region at lower frequencies. The distribution of relaxation times in the vicinity of the glass−rubber relaxation was obtained by a Fourier transformation of the KWW function in the frequency domain and comparison of the moduli in the high-frequency side of the softening region. In this way a β_{KWW} of about 0.25 ± 0.05 was extracted. The shift factors, a_T, were fitted to the well-known Williams−Landel−Ferry (WLF) equation

$$\log a_T = -\frac{c_1^{\,o}(T - T_o)}{c_2^{\,o} + T - T_o} \tag{6}$$

where T_o is a reference temperature and c_1^o and c_2^o are the WLF coefficients at the reference temperature. The following WLF parameters were extracted at T_o: $c_1^o = 10.7$ and $c_2^o = 112$ which correspond to $c_1^g = 19$ and $c_2^g = 63$ at T_g.[5] Notice the c_1^g value is higher than the generally accepted value of 16−17.[32]

Results and Discussion

The structural characteristics within the family of poly(n-alkyl methacrylates) change significantly with the length of the alkyl side chain. In particular, the first sharp diffraction peak, which reflects intersegmental distances, is most affected by increasing the length of the side chain (Figure 4). As we will see below, this change in structural characteristics reflects in their different dynamic behavior. Dielectric spectroscopy identified three processes. At low T, much below T_g, a broad process with the HN shape parameters $\alpha = 0.3$ and $\gamma = 1$ and a strength of $\Delta\epsilon = 3 \times 10^{-2}$ appear in the window of the technique. The T dependence of the relaxation times follows an Arrhenius law

$$\tau = \tau_o e^{E_\gamma/RT} \tag{7}$$

with a high-temperature intercept of $\tau_o = 10^{-15}$ s and an activation energy E_γ of 5.7 kcal/mol. A similar mode was found in PnLMA and was discussed in terms of the

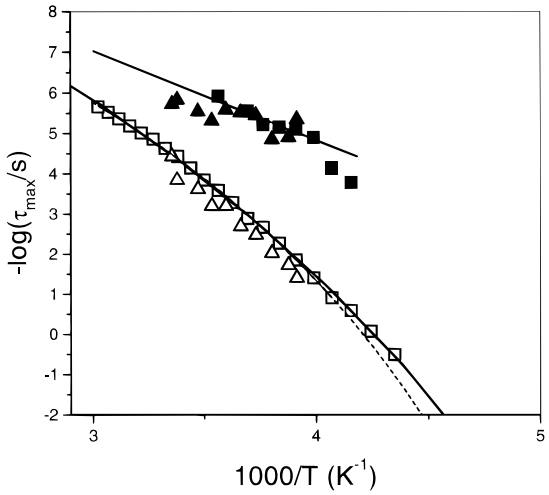

Figure 8. Arrhenius plot of the relaxation times corresponding to the α- (open symbols) and β-relaxation (filled symbols) of PnDMA measured by dielectric spectroscopy (squares) and DLS (triangles). The lines are fits to the dielectric data (see text).

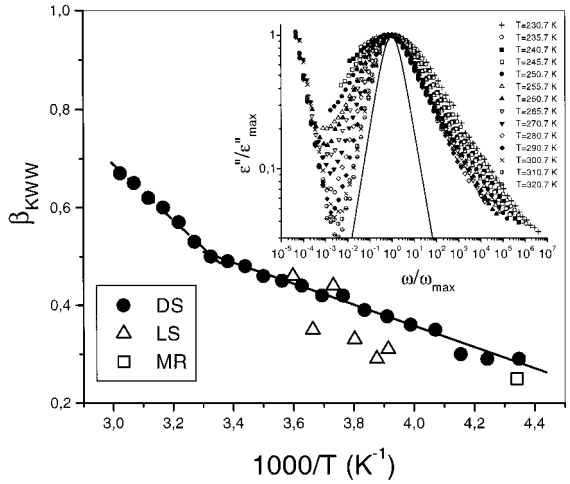

Figure 9. KWW exponent plotted vs inverse temperature for the main α-process. The data from dielectric spectroscopy (●) are compared with those from DLS (△) and rheology (□). In the inset, the normalized dielectric loss data are plotted vs normalized frequency for some temperatures as indicated. The dominant process is the α-relaxation. The process at low frequencies corresponds to the conductivity whereas in the high-frequency side of the main peak the β-relaxation contributes. The solid line represents a Debye process. The α-relaxation is very broad at low T, near T_g, especially from the low-frequency side of the α-peak, and narrows with increasing temperature. Lines are fits to the DS data below and above 300 K.

rotation of the alkyl side group which is mechanically active ($E_\gamma = 5.5$ kcal/mol).[6] At higher temperatures, just above the calorimetric glass transition, there are two dielectrically active modes. The relaxation times of these modes are plotted in Figure 8 in the usual Arrhenius representation. The "fast" process, with an Arrhenius T dependence and with a strength of $\Delta\epsilon_\beta = 6 \times 10^{-2}$, corresponds to a localized hindered rotation of the PE-like side chain with activation parameters ($\tau_o = 2 \times 10^{-5}$ s; $E_\beta = 11.4$ kcal/mol) very much similar to the mechanical γ-relaxation of PE ($E_\gamma = 11$ kcal/mol).[33] The "slow" mode which possess the highest strength from all three modes ($\Delta\epsilon_\alpha = 0.84$ at 290 K), corresponds to the primary ($\alpha\beta$) relaxation with relaxation times described by the Vogel−Fulcher−Tammann (VFT) equation

$$\tau = \tau_o^* e^{B/(T - T_\infty)} \tag{8}$$

where τ_o^*, B, and T_∞ are respectively, the high T intercept, the apparent activation energy, and the "ideal" glass transition temperature ($T_\infty = T_g - c_2^g$). Using the DS data over the whole T range these parameters assume the following values: $\tau_o^* = 10^{-13}$ s, $B = 1570$ K, and $T_\infty = 114$ K. Using only the relaxation times from high temperatures we obtain the more meaningful parameters, as follows: $\tau_o^* = 4 \times 10^{-12}$ s, $B = 1063$ K, and $T_\infty = 144$ K. Only with the last set of parameters did the activation energy B ($=c_1^g c_2^g$) and the ideal glass transition T_∞ ($=T_g - c_2^g$) attain their expected values from the measured WLF coefficients. However, the high-temperature intercept is much longer than the expected phononlike time scale of 10^{-14} s. The cause of this difference might be inherent to the VFT fitting function. It is known that a single VFT fails in describing the dielectric relaxation times of some glass-forming liquids measured over an extended temperature range.[34] However, up to now, there has not been any generally accepted fitting rule of the relaxation times.

In Figure 8, we compare the relaxation times from DS with the ones from DLS. The relaxation times for the primary ($\alpha\beta$) and secondary ("fast" β) processes obtained from DLS have activation parameters similar to the ones from DS; however, the relaxation times for the primary relaxation are systematically slower than those for the same mode probed by DS. The cause of this difference can be the different weighting of the distributions as probed by DS and DLS (first- vs second-order Legendre polynomial).

We discuss next the distribution of relaxation times for the primary ($\alpha\beta$) relaxation. Simple inspection of the dielectric loss data of Figure 3 reveals a pronounced T dependence of the width. To make this more evident we plot in Figure 9 (inset) the same data now normalized to the maximum loss. The spectra show a strong T dependence of the width that is more evident in the low-frequency slope (α parameter of HN function) which changes from 0.4 at 230 K to 0.94 at the highest measurement temperature (330.7 K). Notice that a shoulder appears with increasing T from the high-frequency side, due to the "fast" β-relaxation. To make the comparison of the distribution of relaxation times from the different experiments more quantitative, the following procedure was used: First, the DLS (and rheology) data were fitted directly to the KWW function, and the exponent β_s for the slow process was extracted at some temperatures. To facilitate the comparison with DS we have performed a Fourier transform of the dielectric complex permittivity $\epsilon^*(\omega)$ and fitted the resulting normalized autocorrelation function by the KWW function. This procedure is only an approximation: we extract a single shape parameter in the time domain (β_{KWW}) from spectra which need two shape parameters in the frequency domain (α and γ). Nevertheless, this approximate procedure facilitates the comparison.

The result is shown in Figure 9 where we plot β_{KWW}-(T) for the segmental relaxation from DLS, DS, and rheology. There is generally an agreement between the distributions as obtained from the different experiments; however, the larger errors involved in the DLS analysis preclude a quantitative comparison. The dis-

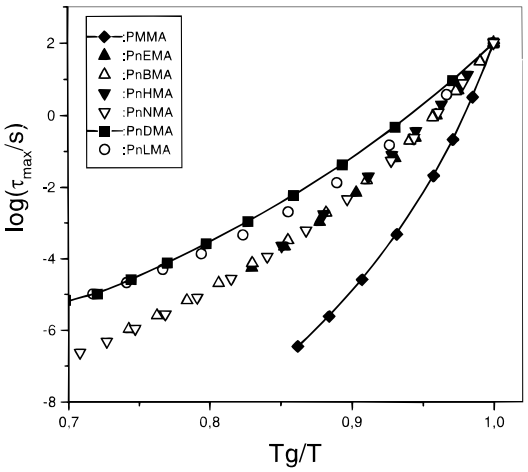

Figure 10. T_g-scaled plot of the segmental relaxation times of PMMA,[16] PnEMA,[8] PnBMA,[8] PnHMA,[21] PnNMA,[8] PnDMA (this work), and PnLMA.[4] The T_g is operationally defined here as the temperature at which the segmental relaxation time is 100 s. There is change in the nature of the glasses when going from PMMA to the higher member of the series which reflects in the change from "fragile" to "strong" behavior.

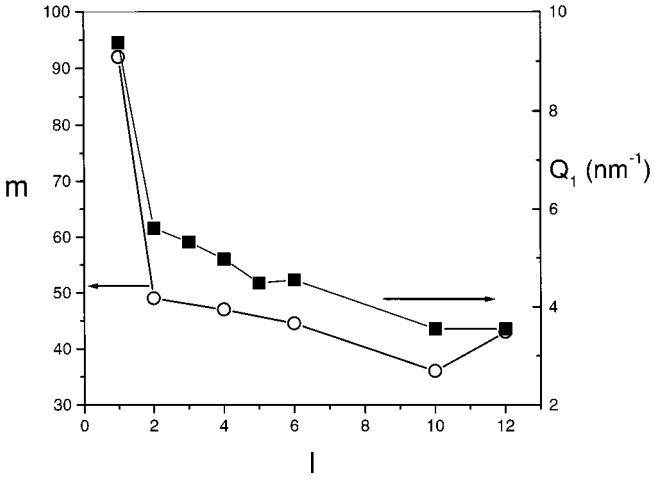

Figure 11. Steepness index m (=d(log τ)/d(T_g/T)), extracted from the initial slopes in Figure 10, plotted as a function of the number of carbon atoms (l) on the side chain of poly(n-alkyl methacrylates). In the same plot the dependence of the low van der Waals peak in the WAXS spectra, Q_1, is shown. There is a one-to-one correspondence between the structural properties and the steepness index, which implies the relation of the fragility to the intersegmental correlations.

tribution of relaxation times obtained from DS is very broad ($\beta_{KWW} \sim 0.3$) at low T near T_g and exhibits a strong T dependence which can be parametrized as $\beta_{KWW}^{T<300K} \sim 1.235 - 220/T$, whereas at $T > 300$ K it is even stronger with $\beta_{KWW}^{T>300K} \sim 2.397 - 569/T$. By extrapolating from the high-temperature side, we obtain $\beta_{KWW} \sim 1$ at $T = 407$ K ($=T_g + 192$ K). PnDMA is therefore one of the few polymers which shows such a narrow ($\beta_{KWW} \sim 0.7$) segmental relaxation even at megahertz frequencies.

A very broad distribution of relaxation times at T_g was also evidenced in PnLMA. This property, which is the norm for all poly(n-alkyl methacrylates) with long side chains, is similar to miscible polymer blends where the segmental α-relaxation is found to broaden considerably as a result of concentration fluctuations.[35−39] The PMMA-like backbone, responsible for the α-relaxation, will encounter a variety of environments due to concentration fluctuations of the PE-like side chains. The concentration fluctuations here result from an intrinsic heterogeneity at the monomer level; the latter is asymmetric both in size and in shape. When the temperature is lowered near the T_g, the dynamic heterogeneity is amplified and results in the broadening of the dispersion. In addition, the primary relaxation in poly(n-alkyl methacrylates) with long side chains is a mixed process and contains the α- and "slow" β-relaxation. The different T dependence of the relaxation times in the two processes contributes to the broad spectra at $T \approx T_g$.

It is interesting now to compare the temperature dependence of the relaxation times of PnDMA with the rest of the members of the series of poly(n-alkyl methacrylates). There is one reservation in this comparison, namely, that the "fragility" is usually defined for homogeneous systems whereas here the monomer itself is intrinsically heterogeneous. However, since for all members of the series there is a single, albeit broad, T_g, we can still compare the $\tau(T)$ from the different samples. For this purpose we employ the usual "fragility plot" where the relaxation times are plotted as a function of reduced temperature (Figure 10). Furthermore, to facilitate the comparison we operationally define T_g as a temperature corresponding to a relaxation time of 100 s. There is a pronounced variation of the curvature or better of the "steepness index" which is defined as

$$m = \frac{\mathrm{d}(\log \tau)}{\mathrm{d}\left(\frac{T_g}{T}\right)} \qquad (9)$$

which is evaluated near T_g, in going from PMMA (with $m \sim 92$) to PnDMA ($m \sim 36$). The variation in m implies a change from a "fragile" to a "strong" liquid, which, in the present case, occurs within the same family of polymers only by increasing the length of the side chain with the addition of a CH_2- unit.

The dynamic behavior within the class of poly(n-alkyl methacrylates) possess the natural question as to whether this dynamic richness reflects on the structural changes and, if so, on what length scale. In other words, are the observed dynamic changes from "fragile" to "strong" reflected on the structural changes? Earlier studies already revealed a correlation between the monomer structure and the degree of intermolecular cooperativity.[3,40,41] To investigate this structure vs dynamics relationship here, we are plotting in Figure 11 both the steepness index m and the position of the LVDW peak as a function of l. In doing so we are directly comparing a dynamic with a structural property. There is a nice correlation between the two quantities, which shows that the observed dynamic changes from "fragile" to "strong" occur by reorganizations at the intersegmental distances which are enlarged by increasing l. It is the first time, to our knowledge, that such a large dynamic change has been quantitatively discussed in terms of a structural change within the same family of polymers and the relevant length scale has been identified. Returning to the potential energy hypersurface as characterizing strong and fragile liquids, the trends observed in poly(n-alkyl methacrylates) would imply a systematic change in the density of minima: from a large number of distinct

minima in PMMA to a small number in PnDMA and PnLMA.

Conclusion

We have investigated the structure and dynamics of poly(*n*-decyl methacrylate) in relation to the other members of the poly(*n*-alkyl methactylate) series. PnDMA shows three relaxation processes, which have been identified as the primary ($\alpha\beta$) relaxation at high T, the "fast" β-relaxation associated with a localized hindered rotation of the PE-like side chain, and, deep into the glassy state, the γ-relaxation, associated with a rotation of the alkyl side group. The distribution of the segmental relaxation times was found to change considerably with temperature and the broadness of the relaxation spectrum near T_g was associated with intrinsic inhomogeneities of the backbone and side chain polymers. A systematic dependence of fragility on the alkyl side chain length was found. This dynamic behavior reflects on the intersegmental distances, which are increasing function of l, as these are probed by the low van der Waals peak of the static structure factor.

Acknowledgment. We thank Prof. T. Pakula for his comments. Partial support to G.F. by the Greek Secretariat for Research and Technology is gratefully acknowledged. P.S. was partially supported by Grant Nos. A4050604 and 12/96/K of the Grant Agency of the Czech Academy of Sciences.

References and Notes

(1) Angell, C. A. In *Relaxation in Complex Systems*; Ngai, K. L., Wright, G. B., Eds.; Naval Research Laboratory: Washington, DC, 1985.
(2) Angell, C. A. *J. Non-Cryst. Solids* **1991**, *131*−*133*, 13.
(3) Bohmer, R.; Ngai, K. L.; Angell, C. A.; Plazek, D. J. *J. Chem. Phys.* **1993**, *99*, 4201.
(4) Floudas, G.; Placke, P.; Stepanek, P.; Brown, W.; Fytas, G.; Ngai, K. L. *Macromolecules* **1995**, *28*, 6799.
(5) Ferry, J. D. In *Viscoelastic Properties of Polymers*, 3rd ed.; Wiley and Sons: New York, 1980.
(6) Heijboer, J.; Pineri, M. In *Nonmetallic Materials and Composites at Low Temperatures*; Hartwig, G., Evens, D., Eds.; Plenum Publ. Co.: New York, 1982.
(7) McCrum, N. G.; Read, B. E.; Williams, G. In *Anelastic and Dielectric Effects in Polymeric Solids*; Dover: New York, 1991.
(8) Ishida, Y.; Yamafuji, K. *Kolloid Z.* **1961**, *177*, 97.
(9) Sasabe, H.; Saito, S. *J. Polym. Sci.* **1968**, *A2*−*6*, 1401.
(10) Williams, G.; Watts, D. C. *Trans. Faraday Soc.* **1971**, *67*, 2793.
(11) Meier, G.; Kremer, F.; Fytas, G.; Rizos, A. *J. Polym. Sci., Polym. Phys.* **1996**, *34*, 1391.
(12) Donth, E.; Beiner, M.; Reissig, S.; Korus, J.; Garwe, F.; Vieweg, S.; Kahle, S.; Hempel, E.; Schroeter, K. *Macromolecules* **1996**, *29*, 6589. Beiner, M.; Korus, J.; Donth, E.; *Macromolecules* **1997**, *30*, 8420.
(13) Fytas, G. *Macromolecules* **1989**, *22*, 211.
(14) Ribes-Greus, A.; Gomez-Ribelles, J. L.; Diaz-Calleja, R. *Polymer* **1985**, *26*, 1849.
(15) Floudas, G.; Fytas, G.; Fischer, E. W. *Macromolecules* **1991**, *24*, 1955.
(16) Floudas, G.; Rizos, A.; Brown, W.; Ngai, K. L. *Macromolecules* **1994**, *27*, 2719.
(17) Patterson, G. D.; Stevens, J. R.; Lindsey, C. P. *J. Macromol. Sci.* **1981**, *B18*, 641.
(18) Meier, G.; Fytas, G.; Dorfmuller, Th. *Macromolecules* **1984**, *17*, 957.
(19) Fytas, G.; Wang, C. H.; Fischer, E. W.; Mehler, K. *J. Polym. Sci., Polym. Phys. Ed.* **1986**, *24*, 1854.
(20) Patterson, G. D.; Jue, P. K.; Stevens, J. R. *J. Polym. Sci.* **1990**, *B28*, 481.
(21) Giebel, L.; Meier, G.; Fytas, G.; Fischer, E. W. *J. Polym. Sci., Polym. Phys. Ed.* **1992**, *30*, 1291.
(22) Kuebler, S. C.; Schaefer, D. J.; Boeffel, C.; Pawelzik, U.; Spiess, H. W. *Macromolecules* **1997**, *30*, 6597.
(23) Stepanek, P. In *Dynamic Light Scattering: The method and some applications*; Brown, W., Ed.; Clarendon Press: Oxford, England, 1993.
(24) Jakes, J. *Collect. Czech. Chem. Commun.* **1991**, *56*, 542.
(25) Rogers, S. S.; Mandelkern, L. *J. Phys. Chem.* **1957**, *61*, 985.
(26) Hempel, E.; Beiner, M.; Renner, T.; Donth, E. *Acta Polym.* **1996**, *47*, 525.
(27) Floudas, G.; Pakula, T.; Stamm, M.; Fischer, E. W. *Macromolecules* **1993**, *26*, 1671.
(28) Miller, R. L.; Boyer, R. F.; Heijboer, J. *J. Polym. Sci., Polym. Phys. Ed.* **1984**, *22*, 2021.
(29) Havriliak, S.; Negami, S. *Polymer* **1967**, *8*, 161.
(30) Karatasos, K.; Anastasiadis, S. H.; Semenov, A. N.; Fytas, G.; Pitsikalis, M.; Hadjicristidis, N. *Macromolecules* **1994**, *27*, 3543. Alvarez, F. Ph.D. Thesis University del Pais Vasco, Spain, 1993.
(31) Provencher, S. W. *Comput. Phys. Commun.* **1982**, *27*, 229.
(32) Angell, C. A. *Polymer* **1997**, *38*, 6261.
(33) Pineri, M.; Berticat, P.; Marchal, E. *J. Polym. Sci., Polym. Phys. Ed.* **1976**, *14*, 1325.
(34) Stickel, F.; Fischer, E. W.; Richert, R. *J. Chem. Phys.* **1955**, *102*, 6251.
(35) Zetsche, A.; Fischer, E. W. *Acta Polym.* **1994**, *45*, 168.
(36) Roland, C. M.; Ngai, K. L. *Macromolecules* **1991**, *25*, 363.
(37) Alegria, A.; Colmenero, J.; Ngai, K. L.; Roland, C. M. *Macromolecules* **1994**, *27*, 4486.
(38) Chung, G.-C.; Kornfield, J. A.; Smith, S. D. *Macromolecules* **1994**, *27*, 5729.
(39) A similar situation for the α-relaxation was found in mixtures of glass-forming liquids studied by dielectric spectroscopy: Shears, M. F.; Williams, G. *J. Chem. Soc., Faraday Trans.*, **1973**, *69*, 608.
(40) Ngai, K. L.; Roland, C. M. *Macromolecules* **1993**, *26*, 6824.
(41) Plazek, D. J.; Ngai, K. L. *Macromolecules* **1991**, *24*, 1224.

MA9804601